PHYSICAL REVIEW E **85**, 025401(R) (2012)

Spectrally peaked electron beams produced via surface guiding and acceleration in femtosecond laser-solid interactions

J. Y. Mao,[1] L. M. Chen,[1,*] X. L. Ge,[1] L. Zhang,[1] W. C. Yan,[1] D. Z. Li,[2] G. Q. Liao,[1] J. L. Ma,[1] K. Huang,[1] Y. T. Li,[1] X. Lu,[1] Q. L. Dong,[1] Z. Y. Wei,[1] Z. M. Sheng,[3] and J. Zhang[1,3]

[1]*Beijing National Laboratory of Condensed Matter Physics, Institute of Physics, Chinese Academy of Sciences, Beijing 100190, China*

[2]*Institute of High Energy Physics, Chinese Academy of Sciences, Beijing 100049, China*

[3]*Department of Physics, Shanghai Jiao tong University, Shanghai 200240, China*

(Received 15 November 2011; revised manuscript received 4 January 2012; published 21 February 2012)

Highly collimated MeV electron beam guiding has been observed along the target surface following the interaction of bulk target irradiation by femtosecond laser pulses at relativistic intensities. The beam quality is shown to depend critically on the laser contrast: With a ns prepulse, the generated electron beam is well concentrated and intense, while a high laser contrast produces divergent electron beams. In the case of large preplasma scale lengths, tunable guiding and acceleration of the target surface electrons is achieved by changing the laser incident angle. By expanding the preplasma scale length to several hundred micrometers, we obtained MeV spectrum-peaked electron beams with a 100 pC per laser pulse and divergence angles of only 3°. This technique suggests a stable method of injection of elections into a variety of accelerator designs.

DOI: 10.1103/PhysRevE.85.025401 PACS number(s): 52.38.Kd, 52.38.Fz

Many groups have reported the observation of collimated electron beams produced by intense laser pulses focused onto solid-density plasmas [1–13], which may be applied, for example, to the fast ignition concept for inertial confinement fusion. For obliquely incident laser pulses producing plasmas at near relativistic intensities, experiments [1–7] and simulations [14–16] have shown that the electron beams are emitted at an angle between laser specular direction and the target normal direction. This emission direction depends critically on the plasma scale length [1,5,7], incident angle [8,9], and laser intensity [10,13], etc. In particular, an electron jet emitted along the target surface [8–11] has been observed using large angles of incidence during laser irradiation of solid targets [8–10]. Recent work has aimed to reveal the operative mechanisms of laser-produced electron emission. For example: Li *et al*. [8] observed that target surface electron beam emission strongly depends on the preplasma condition and the collimated electron beam could only appear when the plasma density scale length is small, while Habara *et al*. [10] considered that higher laser intensity tends to produce electron emission along the target surface. However, in these studies, the target surface electron energy spectrum shows a 100% energy spread [8] and in most cases of laser-solid interaction, the electron spectra are Maxwellian [2,8,9], save for a few recent experiments [4,11,12], where a quasimonoenergetic distribution is obtained with, however, low beam charge and large beam divergence angle.

In the present Rapid Communication, we systematically studied the relationship between the guiding of target surface electrons and laser parameters. As discussed below, when a nanosecond prepulse was added without picosecond amplified spontaneous emission (ASE), the electron beam became concentrated and intense. Guiding of electron jet emission along the target surface was achieved and the divergence angle decreased after increasing the incidence angle. By increasing the preplasma scale length to several hundred micrometers, we obtained a 0.8-MeV quasimonoenergeticlike electron beam with a charge of 100 pC integrated over a single shot and a divergence angle as small as 3° for an electron energy $E_e > 1$ MeV.

The experiments were carried out by using an approximately 240-mJ Ti:sapphire laser working at a center wavelength of 800 nm. The pulse temporal contrast for a picosecond prepulse was around 1×10^{-9} and that for a nanosecond prepulse was around 1×10^{-5}. The experimental layout is shown in Fig. 1. The p-polarized laser beam with a duration of $\tau_0 = 67$ fs was focused by a $f/3.5$ off-axis paraboloidal mirror at an incidence angle of 45°–72°, respectively, onto a thick flat Cu target (a disk of 50 mm diameter and 6 mm thick). The full width half maximum (FWHM) of the laser focal spot was measured to be about 7 μm. For some shots, two prepulses with a maximum intensity of 2×10^{13} W/cm^2 were applied to create preplasmas 7 and 14 ns in advance of the arrival of the main laser pulse. An electron spectrometer with 1000-G magnetic field was set along the target surface direction (approximately within 5° from the target surface) and 147 mm away from the focus spot to measure the electron energy distribution in the range of 5 keV to 2 MeV. Three stacks of image plates (IPs) (Fujifilm BAS-SR 2025, calibrated in Ref. [17]) with a 100-μm-thick aluminum filter, surrounded the laser plasma to record the hot electrons ejected from the plasma. By using the CASINO Monte Carlo program [18], we calculated the energy-dependent depth penetration of electrons into the stack of a filter and IPs. In Fig. 1(a), the stack was composed with an aluminum filter and four pieces of IPs, which could stop electrons whose energy was, respectively, 0.15, 0.5, 0.8, and 1 MeV. In order to measure the preplasma scale length experimentally [19], a single-photon-counting x-ray CCD with a knife edge was used to measure the size and central position of the x-ray source [20]. The NaI detector system was used to measure the γ-ray emission [21] and monitor the laser focus.

At first, we studied the angular distribution of the emitted fast electron jets using incident laser pulses with a low ns temporal contrast. By tuning the laser incident angle to

*lmchen@aphy.iphy.ac.cn

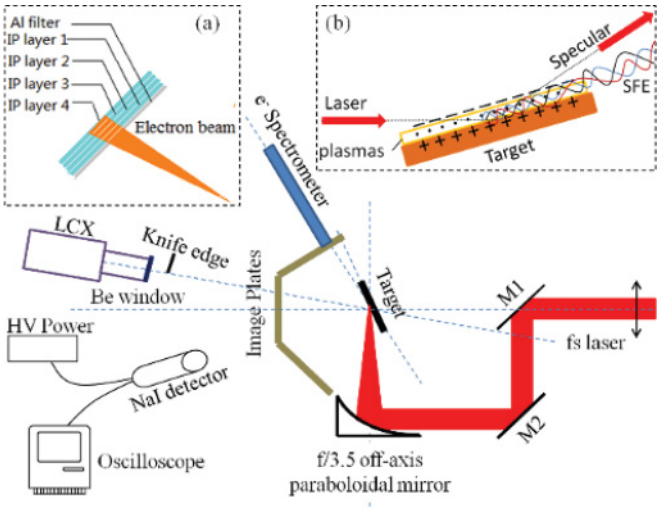

FIG. 1. (Color online) Experimental setup. The angular distribution of the outgoing fast electrons was measured by stacking image plates (IPs) in the target surface direction, laser specular direction, and target normal direction. (a) shows the ejected electrons penetrating a 100-μm aluminum filter and four IPs. (b) exhibits a cartoon of producing surface fast electrons (SFEs).

45°, 67.5°, and 72°, respectively, guiding control of the electron beam along the target surface direction was achieved. Figure 2(a) shows IP images for the case of 45°. Here the emitted electrons in the target surface direction are ejected with a large divergence angle and are not energetic enough to reach the third IP layer. Meanwhile, the emission of electrons in the target normal direction and laser specular direction is relatively intense, as shown clearly in Fig. 2(b). When it comes to the case of 67.5°, the outgoing electrons form two bunches in the laser specular direction and target surface direction. Furthermore, they are more energetic than that in the case of 45°, as shown by the increased penetration in Fig. 2(c); the electron emission in the target normal direction is almost invisible, as seen in Fig. 2(d). In the case where the incident angle is increased to 72°, we observe from Fig. 2(e) that the two bunches of electrons in the case of 67.5° become one beam emitted along the target surface only. The electron beam divergence angle is relatively small (∼3°) and the angular distribution of the electron beam is closer to the target surface direction, as seen in Fig. 2(f). Clearly a large incident angle is more suitable for generating energetic and collimated fast electron jets along the target surface. However, in some cases, if the laser intensity is not high enough, the target surface electron beam becomes divergent and less energetic, according to our experimental observation.

These experimental phenomena concerning laser interactions leading to electron guiding and acceleration along target surfaces could be informed by simulation results related to the betatron oscillation process in Refs. [22–24]. At a large incident angle, two bunches of electrons are observed in the target surface and laser specular directions [22]. Electrons along the target surface are accelerated in the betatron oscillation process while electrons emitted in the laser specular direction are accelerated dominantly by the laser pulses. In the case of laser grazing incidence, intense quasistatic magnetic and electric

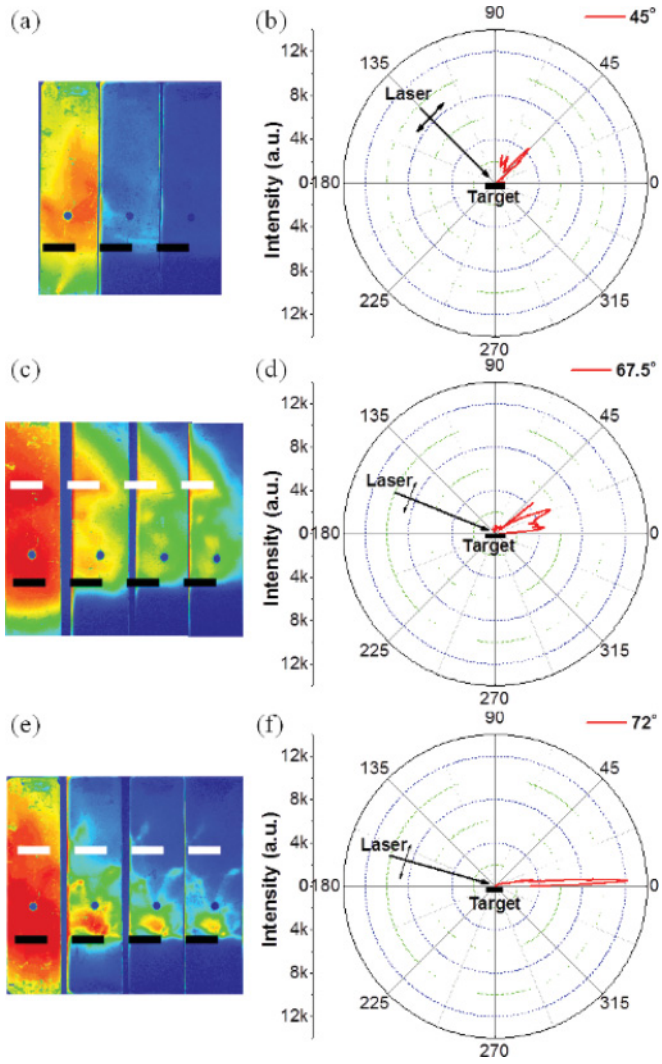

FIG. 2. (Color online) The angular distribution of the target surface electrons emitted from a laser plasma at incident angles of, respectively, 45° [(a) and (b)], 67.5° [(c) and (d)], and 72° [(e) and (f)], with the same color bar. Here IP images in (a), (c), and (e) are from the specific stacks in the target surface and registrations from other stacks in the laser specular, and target normal directions are not shown. The horizontal dashed (upper) lines represent the specular direction, and dashed (lower) lines represent the target surface. The angular distribution in the polar coordinate of emitted electrons is obtained from the signals of the second IP of each stack that subtended both the specular direction and target normal direction. The circles showing up in the IP images are due to holes in the IPs to permit target surface electrons to enter the electron spectrometer.

fields are generated inside the preplasmas on the target surface. Electrons are confined in these combined fields and moving along the target surface with betatron oscillation, as shown in Fig. 1(b). Increasing the incident angle enhances the self-generated electromagnetic fields due to electron current generated along the target surface [23]. In this picture, as the grazing angle increases toward 72°, electron emission that would have followed along the laser specular direction decouples from the bulk plasma and is guided to the target surface, which leads to a more confined divergence angle of electron emission. This phenomenon of the target surface electron generation is also

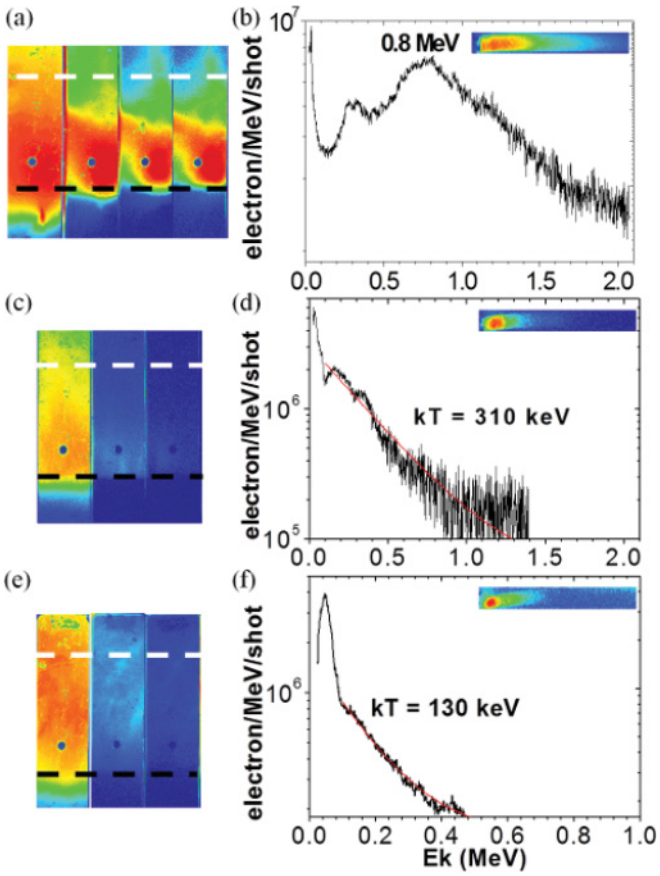

FIG. 3. (Color online) Comparison of the target surface electron angular distribution and the electron energy spectrum, respectively, in low laser contrast with a ns prepulse [(a) and (b)], a high laser contrast without ns prepulse [(c) and (d)], and with a saturable absorber in a low laser contrast situation [(e) and (f)].

assigned by Habara *et al.* [10] under quite different experimental conditions, primarily addressing the influence of laser intensity. Meanwhile, Li *et al.* [8] report that large incident laser angles can also produce fast surface electrons. However, their results have not revealed the gradual dependence of the angular distribution of the electron jet on the laser incident angle. And the electron beam they obtained has a much larger divergence angle ($\sim$15°) [8] than that of this study.

We next systematically studied the target surface electron jet emission dependence upon the laser contrast. Taking the incidence angle of 68.5°, for example, we compared the angular distribution and energy spectrum of the target surface electrons at different prepulse levels. In the case of a ns prepulse $\sim 10^{-5}$, as seen in Fig. 3(a), the electron beam in the target surface direction presented a small divergence angle and high energy ($E_e > 1$ MeV). Meanwhile, in the laser specular direction and the target normal direction, the electrons were too weak to penetrate through the second IP layer. The electron spectrum was obtained in the target surface direction, as shown in Fig. 3(b), which exhibited a double-peak structure. The dominant peak of the spectrum is at about 0.8 MeV and the detectable maximum energy approaches 2 MeV. It reveals that there should be a quasimonoenergeticlike electron bunch generated at an energy of 0.8 MeV. The most reasonable explanation for these phenomena is also considered to be the betatron oscillation process in underdense preplasmas [22,24]. When the frequency of the transverse electron oscillation in the self-generated electromagnetic field is resonantly coupling with the laser frequency, the surface electrons would gain energy efficiently from the laser wave and be accelerated. However, based on particle-in-cell simulations under our experimental conditions, the time evolution of the electron energy spectrum shows that electrons are accelerated at the earlier time. Later they experience deceleration when the laser begins to defocus and the betatron oscillation frequency does not coincide with the laser frequency. In the time-dependent modeling, a peaked electron spectrum is observed and the peak gradually shifts to about 0.8 MeV, which is similar with our experimental results.

Comparing to the situation above, we optimized the laser ns contrast to 10^{-6} by using an ultrafast Pockels cell in the laser system. As seen in Fig. 3(c), the electron beam is not collimated, even still along the target surface. The electron energy spectrum in Fig. 3(d) shows that the electron energy is much lower and exhibits a Maxwellian distribution with an effective temperature $kT = 310$ keV, by fitting the spectrum with the exponential decay. It indicates that the target surface electron guiding process and acceleration critically depends on laser pulse contrast. In order to validate the significance of the ns prepluse for fast electrons generated in the target surface, we repeated the experiments employing a saturable absorber [25] in the laser system to remove the laser ns prepulse and ASE. Qualitatively similar to Fig. 3(c), target surface electrons in Fig. 3(e) are also divergent and even less intense. The energy spectrum also exhibits a Maxwellian distribution with the electron temperature of only $kT = 130$ keV, as shown in Fig. 3(f). Thus, we could conclude that preplasma conditions are critical to the generation of target surface electrons.

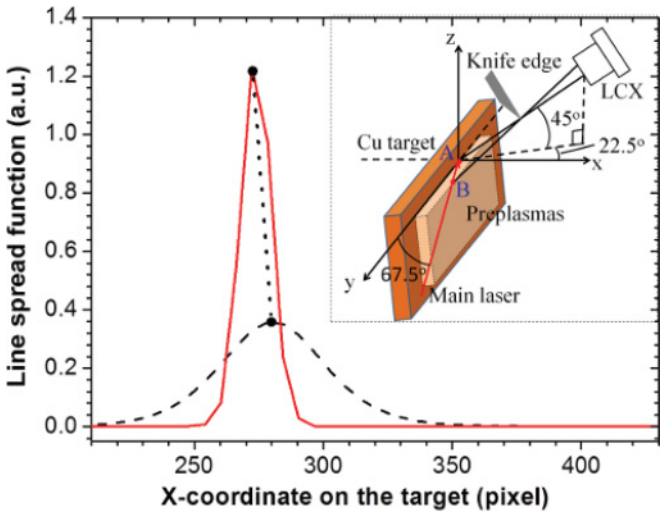

FIG. 4. (Color online) X-ray source position coordinates on target with (dashed black line) and without preplasmas (solid red line). The horizontal axis of the dotted black line represents the difference of the preplasma scale length between these two conditions. The inset is the sketch map of the experimental method [19] to measure the preplasma scale length, where the x-ray source spot is at point A without preplasmas and at point B with preplasmas.

The development of the preplasmas for a laser ns contrast of 10^{-5} and better is calculated by using the ion-acoustic velocity to represent the surface expansion velocity of the preplasmas [26]. The equation in the theory of relativistic plasmas is $C_s = \sqrt{\frac{ZT_e+3T_{io}}{M_{\mathrm{Cu}}}}$ where C_s is the ion-acoustic velocity, Z is the charge state of the ions, T_e is the electron temperature, T_{io} is the initial velocity of the ions, and M_{Cu} is the mass of the ions, assuming the ions are static before interaction ($T_{io} = 0$). According to this equation, we obtain a preplasma scale length which is $\sim$300 μm for a ns laser contrast of 10^{-5} and $\sim$150 μm for a high laser ns contrast. We also used an experimental method [19] to measure the difference of preplasma scale length in the cases of with and without prepulse, which was found to be 145 μm, as shown in Fig. 4. The results achieved by using these two methods match well. In our experiment, the laser pulse with scarce ASE and appropriate prepulse heats the target efficiently and generates the platformlike preplasma of several hundred micrometers. This low-density large-scale preplasma will provide an underdense plasma environment to generate the quasistatic electromagnetic fields [23] that effectively trap the electron beam and guide it along the target surface.

We would like to highlight that after electron beam optimization via using a low ns contrast laser in a large incident angle of 72°, a well-guided spatially and spectrally peaked electron beam is generated along the target surface with, in the case of the present work, a total charge of 100 pC per shot and a divergence angle of 3° ($E_e > 1$ MeV). We noted that Mordovanakis *et al.* [12] also observed monoenergeticlike electron beam jets emitted between the laser specular and target normal directions, with a much larger divergence and producing a much lower total electron charge. In that study, a holelike structure was in the center of the electron beam, which meant that the beam was disturbed by the reflecting laser pulse.

To conclude, we investigated the generation of highly collimated MeV electron beams from the interaction of Cu targets irradiated by a fs laser. The ns laser prepulse is crucial for the generation of the target surface electron beam. With the use of a prepulse, the beam guiding process of the target surface electrons with a small angular divergence is achieved by increasing the laser incident angle. By increasing the preplasma scale length to $\sim$300 μm, which is optimal for beam guiding under these conditions, we achieved MeV quasimonoenergetic accelerated electron jets with a total charge of 100 pC per shot and divergence angle as small as 3°. This electron beam is appropriate to be applied as a stable injector in traditional accelerators, laser-plasma wake field acceleration techniques, or in the utility of a variety of medical applications.

We thank L. T. Hudson at NIST for fruitful discussions. This work was supported by the National Natural Science Foundation of China (NSFC) (Grants No. 60878014, No. 10974249, No. 10735050, No. 10925421, No. 10734130, and No. 10935002).

[1] S. Bastiani, A. Rousse, J. P. Geindre, P. Audebert, C. Quoix, G. Hamoniaux, A. Antonetti, and J. -C. Gauthier, Phys. Rev. E **56**, 7179 (1997).

[2] M. H. Key, M. D. Cable, T. E. Cowan *et al.*, Phys. Plasmas **5**, 1966 (1998).

[3] Y. Sentoku, H. Ruhl, K. Mima, R. Kodama, K. A. Tanaka, and Y. Kishimoto, Phys. Plasmas **6**, 2855 (1999).

[4] T. E. Cowan, M. Roth, J. Johnson *et al.*, Nucl. Instrum. Methods Phys. Res., Sect. A **455**, 130 (2000).

[5] M. I. K. Santala, M. Zepf, I. Watts *et al.*, Phys. Rev. Lett. **84**, 1459 (2000).

[6] Y. T. Li, J. Zhang, L. M. Chen *et al.*, Phys. Rev. E **64**, 046407 (2001).

[7] L. M. Chen, J. Zhang, Y. T. Li *et al.*, Phys. Rev. Lett. **87**, 225001 (2001).

[8] Y. T. Li, X. H. Yuan, M. H. Xu *et al.*, Phys. Rev. Lett. **96**, 165003 (2006).

[9] Z. Li, H. Daido, A. Fukumi *et al.*, Phys. Plasmas **13**, 043104 (2006).

[10] H. Habara, K. Adumi, T. Yabuuchi *et al.*, Phys. Rev. Lett. **97**, 095004 (2006).

[11] L. M. Chen, M. Kando, M. H. Xu *et al.*, Phys. Rev. Lett. **100**, 045004 (2008).

[12] A. G. Mordovanakis, J. Easter, N. Naumova *et al.*, Phys. Rev. Lett. **103**, 235001 (2009).

[13] W. T. Wang, J. S. Liu, Y. Cai *et al.*, Phys. Plasmas **17**, 023108 (2010).

[14] Z. M. Sheng, Y. Sentoku, K. Mima, J. Zhang, W. Yu, and J. Meyer-ter-Vehn, Phys. Rev. Lett. **85**, 5340 (2000).

[15] H. Ruhl, Y. Sentoku, K. Mima, K. A. Tanaka, and R. Kodama, Phys. Rev. Lett. **82**, 743 (1999).

[16] R. Kodama, K. A. Tanaka, Y. Sentoku *et al.*, Phys. Rev. Lett. **84**, 674 (2000).

[17] K. A. Tanaka, T. Yabuuchi, T. Sato, R. Kodama, Y. Kitagawa, T. Takahashi, T. Ikeda, Y. Honda, and S. Okuda, Rev. Sci. Instrum. **76**, 013507 (2005).

[18] D. Drouin, A. R. Couture, D. Joly, X. Tastet, V. Aimez, and R. Gauvin, Scanning **29**, 92 (2007).

[19] L. M. Chen, P. Forget, S. Fourmaux, J. C. Kieffer, A. Krol, C. C. Chamberlain, B. X. Hou, J. Nees, and G. Mourou, Phys. Plasmas **11**, 4439 (2004).

[20] M. H. Xu, L. M. Chen, Y. T. Li *et al.*, Acta Physica Sinica **56**, 1 (2007).

[21] P. Zhang *et al.*, Phys. Rev. E **57**, R3746 (1998).

[22] M. Chen, Z. M. Sheng, J. Zheng, Y. Y. Ma, M. A. Bari, Y. T. Li, and J. Zhang, Opt. Express **14**, 3093 (2006).

[23] T. Nakamura, S. Kato, H. Nagatomo, and K. Mima, Phys. Rev. Lett. **93**, 265002 (2004).

[24] A. Pukhov, Z. M. Sheng, and J. Mayer-ter-Vehn, Phys. Plasmas **6**, 2847 (1999); C. Gahn, G. D. Tsakiris, A. Pukhov, J. Mayer-ter-Vehn, G. Pretzler, P. Thirolf, D. Habs, and K. J. Witte, Phys. Rev. Lett. **83**, 4772 (1999).

[25] M. Nantel, J. Itatani, A. C. Tien *et al.*, IEEE J. Sel. Top. Quantum Electron. **4**, 449 (1998).

[26] F. N. Beg, A. R. Bell, A. E. Dangor, C. N. Danson, A. P. Fews, M. E. Glinsky, B. A. Hammel, P. Lee, P. A. Norreys, and M. Tatarakis, Phys. Plasmas **4**, 447 (1997).